

Lactate vs butyrate production during mixed culture glucose fermentation driven by substrate availability as determined by metaproteomics

Robert Hoelzle¹, Daniel Puyol¹, Bernardino Viridis¹, and Damien Batstone¹

¹The University of Queensland

August 11, 2020

Abstract

Mixed-culture fermentation provides a means to recycle carbon from complex organic waste streams into valuable feedstock chemicals. Using complex microbial consortia, individual systems can be tuned to produce a range of biochemicals to meet market demand. However, the metabolic mechanisms and community interactions which drive product expression changes under differing conditions are currently poorly understood. Furthermore, predictable product transitions are currently limited to pH-driven changes between butyrate and ethanol, and chain-elongation (fed by CO₂, acetate, and ethanol) to butyrate, valerate, and hexanoate. Lactate, a high-value biopolymer feedstock chemical, has been observed in transition states, but sustained production has not been described. In this work, a continuous stirred bioreactor was operated at low pH (5.5) with substrate concentration varied between limiting and non-limiting conditions. Using glucose as a model substrate, two sustained operational states were defined: butyrate production during substrate limitation, and lactate production in the non-limited state. Through SWATH-MS metaproteomics and 16S rDNA community profiling, the mechanism of change between butyrate and lactate was described primarily by redirected carbon flow through the methylglyoxal bypass by *Megasphaera* under substrate non-limiting concentrations. Crucially, butyrate production resumed upon return to substrate-limited conditions, demonstrating the reversibility of this transition.

Lactate vs butyrate production during mixed culture glucose fermentation driven by substrate availability as determined by metaproteomics

Advanced Water Management Centre, The University of Queensland, Brisbane, Qld 4072, Australia

Australian Centre for Ecogenomics, The University of Queensland, Brisbane, Qld 4072, Australia

School of Earth and Environmental Sciences, The University of Queensland, Brisbane, Qld 4072, Australia

Group of Chemical and Environmental Engineering, King Juan Carlos University, 28933 Móstoles, Madrid, Spain

*Correspondence should be addressed to: Robert D. Hoelzle, School of Earth and Environmental Sciences, The University of Queensland, St. Lucia, QLD 4072, Australia Phone: +61 7 3365 2108; Fax: +61 7 3365 6899; E-mail: r.hoelzle@uq.edu.au

Abstract

Mixed-culture fermentation provides a means to recycle carbon from complex organic waste streams into valuable feedstock chemicals. Using complex microbial consortia, individual systems can be tuned to produce a range of biochemicals to meet market demand. However, the metabolic mechanisms and community

interactions which drive product expression changes under differing conditions are currently poorly understood. Furthermore, predictable product transitions are currently limited to pH-driven changes between butyrate and ethanol, and chain-elongation (fed by CO₂, acetate, and ethanol) to butyrate, valerate, and hexanoate. Lactate, a high-value biopolymer feedstock chemical, has been observed in transition states, but sustained production has not been described. In this work, a continuous stirred bioreactor was operated at low pH (5.5) with substrate concentration varied between limiting and non-limiting conditions. Using glucose as a model substrate, two sustained operational states were defined: butyrate production during substrate limitation, and lactate production in the non-limited state. Through SWATH-MS metaproteomics and 16S rDNA community profiling, the mechanism of change between butyrate and lactate was described primarily by redirected carbon flow through the methylglyoxal bypass by *Megasphaera* under substrate non-limiting concentrations. Crucially, butyrate production resumed upon return to substrate-limited conditions, demonstrating the reversibility of this transition.

Keywords

Lactate production; butyrate; mixed-culture fermentation; metabolic regulation; carbon recycling

Introduction

Fermentation is a key central step in biologically treating organic waste in which waste carbon can be recycled into valuable short-chain fatty acids, alcohols, and other organic (bio)chemicals (Agler, Wrenn, Zinder, & Angenent, 2011; Angenent et al., 2016; De Groof, Coma, Arnot, Leak, & Lanham, 2019). While the definition is not universally agreed upon, fermentation can generally be described as biological catabolism without the use of an external electron acceptor (such as O₂, NO₃⁻, or SO₄²⁻), and commonly relies on substrate-coupled electron transfer reactions for energy generation (El-Mansi, Bryce, Demain, & Allman, 2006). As such, microbes have evolved a variety of metabolic pathways to balance their carbon and electron loads (Hoelzle, Viridis, & Batstone, 2014). These pathways generate the variety of chemical products inherent to fermentation.

Angenent et al. (2004), Spirito et al. (2014), and Hoelzle et al. (2014) identified several advantages of fermentation by mixed cultures, or natural consortia of microbes, over defined cultures. Key among these are 1. diverse mixed cultures provide a range of metabolic functional clades, which allows flexibility to consume a wide variety of substrates; 2. functional redundancy between disparate microbial groups ensures production robustness toward substrate contaminations and process disturbances; and 3. reduced equipment and operational costs due to lack of need to sterilize.

To date, research on mixed-culture fermentation (MCF) has primarily focused on carbohydrate-based pH-driven processes, which produce primarily acetate and butyrate at low pH and acetate and ethanol at high pH (Atasoy, Eyice, Schnürer, & Cetecioglu, 2019; Lu, Slater, Mohd-Zaki, Pratt, & Batstone, 2011; Mohd-Zaki et al., 2016; M F Temudo, Muyzer, Kleerebezem, & van Loosdrecht, 2008; Margarida F. Temudo, Mato, Kleerebezem, & Van Loosdrecht, 2009; Margarida F Temudo, Kleerebezem, & van Loosdrecht, 2007), and chain elongation of syngas fermentation products, which produces hexanoate and caprylate (Dams et al., 2018; Kucek, Spirito, & Angenent, 2016; Spirito, Marzilli, & Angenent, 2018; Spirito et al., 2014). While these production modes have proven reproducible, these products represent only a limited range of possible MCF-generated biochemicals (Hoelzle et al., 2014; Jang et al., 2012). For instance, reproducible MCF production modes have not been described for lactate and propionate, which are higher-value products used to produce biopolymers such as polylactic acid (PLA), poly(glycolate-co-lactate-co-3-hydroxybutyrate), and as a precursor to polyhydroxyalkanoates (PHA), as well as vinyl propionate respectively. Instead, these products are currently produced in pure-culture fermentation systems (Alves de Oliveira, Komesu, Vaz Rossell, & Maciel Filho, 2018; Gonzalez-Garcia et al., 2017; Hofvendahl & Hahn-Hagerdal, 2000). However, lactate in particular has been observed as a major product during transient states and periods of increased substrate loading in anaerobic digestion (to methane), a process in which MCF is the generating step for methanogenic substrates (Eng, Fernandes, & Paskins, 1986; Romli, Keller, Lee, & Greenfield, 1995). This suggests that high substrate concentration could act as a control for lactate formation in MCF, potentially

opening up more economical methods of production.

In order to control the production of a given biochemical, it is necessary to understand the underlying community assembly dynamics and metabolic mechanisms which result in its production. Gonzalez-Cabaleiro et al. (2015) have developed a metabolic model for the pH-driven substrate-limited system which successfully describes the acetate-butyrate to acetate-ethanol switch based on electron balancing and modes of active product transport across the cell membrane. Advancements in meta-omics approaches now make it possible to describe these determinative factors through observed changes in gene expression and protein formation (Grobler et al., 2014; Matallana-Surget, Jagtap, Griffin, Beraud, & Wattiez, 2017; Singleton et al., 2018; Wang & Kuruc, 2019; Woodcroft et al., 2018).

In this research, high substrate concentration is explored as a control strategy for alternative MCF production modes by transitioning between substrate-limited and substrate non-limited conditions. Furthermore, community assembly dynamics and functional metabolic expression are described through a combination of 16S rDNA amplicon community profiling and SWATH-MS metaproteomics.

Materials and Methods

2.1. Experimental approach

A continuous flow stirred-tank bioreactor (Supplementary Fig. 1) was operated for 22 weeks under a range of substrate concentrations using glucose as a model substrate. Initial operation matched previously reported conditions for acetate-butyrate production with substrate concentration limited at $5 \text{ g}_{\text{glu}}^* \text{L}^{-1}$, hydraulic retention time fixed at 1 day, pH at 5.5 and, temperature at 30degC (Lu, Slater, Mohd-Zaki, Pratt, & Batstone, 2011; Mohd-Zaki et al., 2016; M F Temudo, Muyzer, Kleerebezem, & van Loosdrecht, 2008; Margarida F Temudo, Kleerebezem, & van Loosdrecht, 2007). Though conditions for both acetate-butyrate and acetate-ethanol production modes have previously been described, acetate-butyrate was chosen as the base production mode on the hypothesis that the lower electron sinking capacity of butyrate compared to ethanol production offers greater potential for expression of alternative pathways for electron mediation (Hoelzle et al., 2014). Full description of bioreactor setup and control is provided in the Supplementary Methods.

The bioreactor was sampled for product composition every 2-4 days. After establishment of steady state acetate-butyrate production (as evidenced by a <10% variation in the 2 primary products over 3 consecutive samples), sampling was expanded to include microbial community structure and protein expression over the next 6 samples (~1.5 weeks). After initial steady state operation, the substrate feed concentration was increased from 5 to $10 \text{ g}_{\text{glu}}^* \text{L}^{-1}$, then to 15, 20, and finally back to $5 \text{ g}_{\text{glu}}^* \text{L}^{-1}$, establishing steady state operation at each concentration. Hence loading rates ranged from 5 to $20 \text{ g}_{\text{glu}}^* \text{L}^{-1} \text{d}^{-1}$.

Due to a failed extraction from one of the protein samples (third sample of fifth steady state period), protein analysis was limited to 5 randomly selected samples per steady state period. 16S rDNA amplicons were then sequenced for samples matching the first, third, and final protein samples (Supplementary Table 1). Product composition was then correlated to the community and protein expression analyses to describe the response at a metabolic level at each steady state loading rate.

2.2. Media

Biomass was activated overnight in tryptone-glucose-yeast extract medium before inoculating into freshwater basal anaerobic (BA) media (Bastidas-Oyanedel, Mohd-Zaki, Pratt, Steyer, & Batstone, 2010; Widdel & Bak, 1992). The reactor was then fed with BA media as described above.

A separate tryptone-glucose-yeast extract (TGY) medium was used for culture activation before inoculation into the bioreactor. Details on media preparation are available in the Supplementary Methods.

2.3. Inoculum

A diverse mixed culture was required in order to ensure exploration of the interacting effects between a variety of microbial functional groups. Granules from the upflow anaerobic sludge blanket digester reactor at Golden Circle Cannery in Brisbane, Australia were chosen as the inoculation community. This digester reactor is fed on carbohydrate-rich fruit and vegetable canning wastewater.

The granules were collected less than 48 hours before beginning the experiment. To activate the community, granules were crushed in a plastic bag by hand using a roller in order to break up the granule structure while not affecting community composition (Juste-Poinapen, Turner, Rabaey, Viridis, & Batstone, 2015). The crushed granules were then injected at 2% v/v into TGY media, then activated overnight at 30degC. Activated culture was then inoculated into the bioreactor at 1% v/v. The bioreactor pH was adjusted to 7.0, and then continuous feed began once the pH decreased to 5.5.

To ensure continuation of the same culture throughout the experiments, broth samples were taken at weekly intervals from the fermenter and stored in 20% glycerol at -80degC in 2.0 mL aliquots. In the event of reactor failure, the reactor was re-started from the most recent broth sample, activated overnight in TGY media.

2.4. Analytical Methods

2.4.1. Metabolite Analysis

Substrate and product metabolites were determined by HPLC (1050 Series, Hewlett-Packard, USA). 2.0 mL broth samples were first centrifuged at 10,000 x g for 10 min. The supernatant was then passed through a sterile 0.22 μm filter to remove remaining cell mass. Filtered supernatant was then mixed 3:1 with 0.02 N H_2SO_4 (making 0.005 N), and analyzed via HPLC using a 7.7x300 mm Hi-Plex H column with associated guard column and inline filter (Agilent, USA) heated to 40.0°C (TC-50/CH-30, Eppendorf, Germany). The mobile phase was 0.005 N sulfuric acid at 0.800 mL \cdot min $^{-1}$ and the sample injection volume was 30 μL . Products were detected via RID (1047, Hewlett-Packard, USA) at 30°C and a detection range of 32×10^{-5} RIU.

Complete carbon product composition was confirmed by balancing measured and theoretical chemical oxygen demand (COD), a measure of oxidation state. Measured COD of soluble components (SCOD), was determined by COD Cell Test (14555, Merck Millipore, MA, USA) and measured on a Spectroquant® Move 100 colorimeter (Merck Millipore, MA, USA). SCOD measurements used the same samples as those for HPLC measurement. Theoretical COD was calculated from HPLC-measured concentrations based on complete oxidation stoichiometry.

2.4.2. 16S rDNA Amplicon Sequencing

The community profile was assessed 3 times per steady state period, aligned with the first, middle, and final protein samples. DNA was extracted from the cell pellet generated during chemical analysis centrifugation. The pellet was first washed in 2.0 mL of 4°C PBS solution and centrifuged again at 10,000 x g for 10 min. The supernatant was discarded and the pellet was resuspended again in 1.0 mL of PBS, and samples were stored at -20°C until DNA extraction. DNA was extracted using the FastDNA SPIN Kit for Soil (MP Biomedicals, Santa Ana, California) via the manufacturer's protocol. Illumina sequencing of the 16S rDNA gene, PCR amplified using iTAG 16S 926F and 1392wR primers (Engelbrektson et al., 2010), was then performed by the Australian Centre for Ecogenomics (The University of Queensland, Brisbane, Australia).

2.4.3. Protein Extraction and SWATH-MS

Proteins were assessed 5 times per steady state period. Biomass was prepared similarly to the amplicon samples. Final resuspension was in 500 μL of protein extraction solution, which consisted of 77 mg dithiotheretol and 1 tablet of cComplete™ Protease Inhibitor Cocktail (Roche, Switzerland) dissolved into 10.0 mL of B-PER II (Thermo Fisher Scientific Inc, USA). Extraction solution was stored in the dark at 4°C and used within 48 hours. Proteins were extracted and analyzed via SWATH-MS using the method described by Grobber et al. (2014). All samples were prepared for MS analysis at equivalent total protein concentrations. A portion of each prepared sample was mixed into a pooled sample for protein identification.

2.5. Bioinformatics

2.5.1. Community Profiling

Community structure was determined from amplicon reads using QIIME 2 v2017.10 (Caporaso et al., 2010). Lineages (features) were generated using ‘deblur’, with reads truncated to 225 base pairs, then evenly rarefied based on the lowest sample lineage count using ‘feature-table rarefy’. Read alignments were manually verified (Supplementary Note 1, Supplementary Figs. 2 and 3), then blasted against the Silva 132 database at 99% similarity using ‘feature-classifier’ to generate taxonomic labels, which were truncated at the genus level.

The heatmap and dendrogram were generated in R using the pheatmap package from square-root transformation of the genus-aggregated relative lineage abundance data, averaged for each operational level. Shannon diversity index was calculated in R from the whole lineage profile for each sample via the ‘diversity’ function of the vegan package.

2.5.2. Metaproteomics

Proteins were identified from the pooled sample in ProteinPilot (v5.0, SCIEX, Framingham, MA, USA) using a reference proteome consisting of all bacteria, archaea, and fungi on the UniProt database (Bateman et al., 2015). Ion fragments from individual samples were then mapped to identified proteins in PeakView (v2.1, SCIEX, Framingham, MA, USA) at 5 peptides per protein, 3 transitions per peptide, 99% peptide confidence threshold, 1.0% global false discovery rate threshold (calculated in ProteinPilot using the Paragon algorithm), 5.0 min XIC extraction window, and 50 ppm XID width.

Identified proteins were assigned functionality (i.e. amino acid synthesis, butyrate synthesis, etc) based on UniProt listing, and taxonomy was aggregated to genus for consistency with the community profile. Ion intensity tables from PeakView were converted to the “label free LCMS” 10-column table format for processing in MSstats v3.3.12 (Choi et al., 2014).

Raw ion data was processed in MSstats using ‘dataProcess’ with default settings. The default normalization setting in MSstats equalizes the median protein signals across samples. This effectively weights the expression analysis toward taxa with greater representation in the sample. To account for this, functional expression of the proteome was assessed individually by genus. Raw mass spec intensity data was grouped by genus before processing through ‘dataProcess’. The ‘groupComparison’ function was then used to compare expression, measured as log₂-fold change (L2FC), between different levels or groups of levels as described in the text. After expression analysis within individual genera, results were regrouped and assessed by metabolic function. Adjusted $p < 0.05$ was used to define significant differences in expression between comparison groups.

2.6. Statistical Methods

2.6.1. 95% Confidence Intervals

95% confidence intervals were calculated via the following equation:

$$CI_{95} = \pm t_{0.025, n-1} \times \frac{\sigma}{\sqrt{n}} \text{Eq. 1}$$

Where σ and n are the standard deviation and number of samples, respectively. For proteomics data, standard error (SE) from the ‘groupComparison’ function of MSstats was used in place of $\sigma \cdot (\sqrt{n})^{-1}$.

2.6.2. Analysis of Covariance

Product composition was normalized by %SCOD, and then compared between operational levels by analysis of covariance (ANCOVA) via the ‘aov’ function in R, with time from the start of steady state as the covariant. Adjusted p-values and 95% confidence intervals were then calculated using ‘TukeyHSD’ in R.

2.6.3. Canonical Correlation Analysis

Canonical correlation analysis (CCA) was used to assess correlations between metabolite, community profile, and metaproteomic datasets. CCA was carried out in R using the ‘cca’ function of the vegan package. Me-

tabolite analyses used the %COD-normalized profile, community profile analyses used the genus-aggregated relative abundance profile, and metaproteome analyses used “Abundance” data from the ‘dataProcess’ function of MSstats, which was averaged together for each individual metabolic pathway or function.

Results

3.1. Steady State Product Analysis

Steady state was achieved at all operation levels after 1-2 weeks of transitional operation (Supplementary Fig. 4). Initial operating conditions (5 and 10 $\text{g}_{\text{glu}}\cdot\text{L}^{-1}$) produced acetate and butyrate as the major products (Fig. 1), consistent with previous studies (Atasoy, Eyice, Schnürer, & Cetecioglu, 2019; Lu et al., 2011; Mohd-Zaki et al., 2016; M F Temudo et al., 2008; Margarida F Temudo et al., 2007). This product profile will be referred to as “HBu-type”. Production then transitioned to acetate and lactate as the major products, or “HLA-type”, at 15 and 20 $\text{g}_{\text{glu}}\cdot\text{L}^{-1}$. HBu-type fermentation corresponded with complete glucose consumption (Table 1), making this a substrate-limited condition. By contrast, HLA-type fermentation corresponded with incomplete glucose consumption, making this a substrate non-limited condition. Importantly, HBu-type fermentation was regained when the substrate concentration was reduced from 20 $\text{g}_{\text{glu}}\cdot\text{L}^{-1}$ back to 5 $\text{g}_{\text{glu}}\cdot\text{L}^{-1}$, showing reversibility of the production types. Theoretical COD of the product composition balanced to between 90-110% of measured SCOD except for level 15, which balanced to $111\pm 1\%$, confirming measurements of all major products.

ANCOVA comparison of normalized product composition between operational levels revealed that butyrate and acetate production in the first 5 $\text{g}_{\text{glu}}\cdot\text{L}^{-1}$ condition (L5a) were significantly different ($p < 0.05$) than the other two HBu-type levels (Supplementary Table 2). In addition to high acetate and butyrate composition, L5a also had high hexanoate composition ($10\pm 4\%$). For the remainder of the levels, including the second 5 $\text{g}_{\text{glu}}\cdot\text{L}^{-1}$ level (L5b), hexanoate was produced only as a minor product. This initial 5 $\text{g}_{\text{glu}}\cdot\text{L}^{-1}$ condition will therefore be assessed as a separate operational mode from the other HBu-type levels.

No products were produced significantly differently between the 15 $\text{g}_{\text{glu}}\cdot\text{L}^{-1}$ and 20 $\text{g}_{\text{glu}}\cdot\text{L}^{-1}$ conditions. These will therefore be discussed jointly as the “High” levels based on substrate concentration. For the second 5 $\text{g}_{\text{glu}}\cdot\text{L}^{-1}$ (L5b) and 10 $\text{g}_{\text{glu}}\cdot\text{L}^{-1}$ conditions, minor products formate, propionate, and valerate were produced significantly differently. However, major products butyrate and acetate, as well as the remaining minor products, were not produced significantly differently. These operational levels will therefore also be discussed jointly as the “Low” levels. Interestingly, production of formate and propionate were not significantly different between levels 5a and 5b. This may indicate that formate is most readily produced at very low organic loading rates, while propionate is most readily produced at higher organic loading rates.

3.2. Taxonomic Analysis

Dominant lineages across all operational levels were from the genera *Bifidobacterium*, *Ethanoligenens*, *Megasphaera*, *Pectinatus*, and *Dokdonella*, and microbial communities from the Low and High levels were each more similar internally than to each other or to L5a (Fig. 2). *Clostridium* lineages were generally more abundant in the Low and High levels than in L5a, while L5a had higher abundances of lineages from *Olsenella* and the order *Bacteroidales*.

Three separate aggregated genera individually make up at least 20% of the community in at least one operational condition: *Megasphaera*, *Ethanoligenens*, and *Bifidobacterium*. Individual *Megasphaera* lineages (Supplementary Fig. 5) were more abundant in the Low levels ($9.6\pm 0.9\%$ average lineage abundance) than in the High levels ($3.0\pm 0.7\%$) and L5a ($6\pm 1\%$), and combined made up the dominant group in both L5a and the Low levels (25% and 38% summed abundance of lineages, respectively). *Ethanoligenens* lineages were more abundant in the High levels ($7\pm 1\%$) than in the Low levels ($2.3\pm 0.5\%$). They were overall similarly abundant in L5a and the High levels, though a low abundance third lineage resulted in high variance ($6\pm 13\%$). Combined, *Ethanoligenens* lineages made up the defining major group in the High levels (20%). *Bifidobacterium* lineages made up the most abundant group in the High levels at a combined 27%, though

they were similarly abundant in L5a and the Low and High levels at $3\pm 3\%$, $4\pm 2\%$, and $7\pm 4\%$, respectively. Though different lineages were dominant under different conditions, all of the conditions maintained similar community diversity, ranging from 3.15 in L20 to 3.45 in L5b.

3.3. Metaproteomic Analysis

SWATH-MS analysis identified 2565 peptide ions, which mapped to 383 positively identified proteins from 44 genera (Supplementary Data). In order to verify comparisons between 16S rDNA-based and protein-based taxonomic assignments, the genus-aggregated community and metaproteomic abundance profiles were assessed together via CCA (Fig. 3). The greatest proportion of co-variance between these data sets (38.8%, CCA 1) is explained by changes in lineage abundance between the Low and High levels, confirming the taxonomic assignments. This could indicate that the primary variation in measured protein expression is due to changes in lineage abundance. However, this trend in covariance does not extend to CCA 2, likely due to high expression of metabolic versus structural proteins in the varying conditions. In order to eliminate lineage abundance effects on protein expression analysis, further metaproteomic assessments were analyzed separately within each genus. (Supplementary Fig. 6).

After grouping proteins by metabolic function (Supplementary Table 3), those involved in carbon energy metabolism were assessed for L2FC expressional differences between the Low and High levels (Fig. 4). Consistent with the high butyrate production in the Low levels, all significant up-expression of proteins from the acetyl-CoA-to-butyrate pathway was in the Low levels, and these were exclusively from *Megasphaera*. Proteins from both propionate pathways were also generally more up-expressed in the Low levels (from *Megasphaera*, *Anaerovibrio*, and *Megamonas*) than in the High levels (*Dorea*), as were proteins from glycerol production (*Megasphaera*) and consumption (*Clostridium*). The majority of electron mediating cofactors (EMCs) were up-expressed in the Low levels by *Megasphaera*, though this function was up-expressed in the High levels by *Bifidobacterium*.

In the High levels, where acetate and lactate were more highly produced, proteins from these pathways were generally more up-expressed than in the low levels. This is especially true for the methylglyoxal bypass pathway of lactate production in *Megasphaera*, which despite this genus being more than 3x lower abundance in the High levels, up-expressed glyoxalase by 5.2 ± 0.2 L2FC.

Consistent with the higher substrate load in the High levels, proteins for central carbon metabolism (glycolysis and the pentos-phosphate pathway) were generally more up-expressed in the High levels from a variety of lineages, especially *Clostridium*, *Bifidobacterium*, and *Ethanoligenens*. Yet, overall proteins for substrate uptake, such as ABC-type and PTS system sugar transporters, were roughly equally as up-expressed in both High and Low levels. Expression of substrate uptake proteins does vary by lineage, however, with *Megasphaera* more active in the High levels (again, despite lower abundance) and *Clostridium* more active in the Low levels.

Discussion

4.1. Product Spectrum and Community Profile

The HBU-type MCF production mode has been well-established at low pH and substrate-limited conditions in previous research (Lu et al., 2011; Margarida F Temudo et al., 2007), and a metabolic control mechanism for the transition between high and low pH has been proposed and supported in models (Gonzalez-Cabaleiro et al., 2015; Rodriguez, Kleerebezem, Lema, & van Loosdrecht, 2006). While high organic loading rate has been proposed as a mechanism to promote chain elongation (De Groof et al., 2019), elevated production of reduced acid products such as lactate and propionate has only been reported during transition states (Eng et al., 1986; Voolapalli, 2001). Sustained HLa-type MCF production has not previously been reported, nor has the metabolic mechanism been described for transition to this production state.

A typical community profile assessment of the production data, such as those reported by Mohd-Zaki et al. (2016) and Atasoy et al. (2019), shows that the defining product spectrum can largely be attributed to the

major taxonomic lineages within each operational condition. Butyrate and acetate are primary products of *Megasphaera* (Marounek, Fliegerova, & Bartos, 1989; Weimer & Moen, 2013), *Pectinatus* (Watier, Dubourguier, Leguerinel, & Hornez, 1996), and *Bifidobacterium* (de Vries & Stouthamer, 1968; Wolin, Zhang, Bank, Yerry, & Miller, 1998), while lactate and acetate are primary products of *Bifidobacterium* and *Ethanoligenens* (Castro, Razmilic, & Gerdtzen, 2013; Xing et al., 2006). However, what is not clear from the metabolite and community profile datasets alone is why the community transitions from predominantly *Megasphaera* and *Bifidobacterium* to *Ethanoligenens* and *Bifidobacterium*. Our metaproteome analysis offers insights into the metabolic mechanisms which generate this transition, and therefore the transition to HLa-type production. We begin with an assessment of the HBU-type to HLa-type transition by comparing the Low and High levels, then follow with a brief analysis of the apparent outlier L5a condition.

4.2. Change in Pathway Expressions between Low and High Levels

Upon plotting pathway expression on a model MCF metabolic network (Hoelzle et al., 2014), it is evident that, consistent with the total protein expression profile, *Megasphaera* accounts for most of the up-expressed pathways in the Low levels, while *Bifidobacterium* and *Ethanoligenens* account for most up-expressed pathways in the High levels (Fig. 5). *Clostridium* is the exception, with the total protein expression profile suggesting it should be most active in the High levels. However, the majority of the High level up-expressed *Clostridium* enzymes are related to biomass synthesis (Supplementary Table 3), while the carbon metabolism enzymes are generally more highly expressed in the Low levels.

The trends in pathway expression align with the trends of product expression, though no enzymes for ethanol production were detected, while enzymes for formate production, detected in *Bifidobacterium*, did not significantly change expression. *Megasphaera* was responsible for high butyrate production in the Low levels, having up-expressed enzymes for the acetyl-CoA-to-butyrate pathway. The increased acetate production in the High levels was due to increased expression of the acetyl-CoA-to-acetate pathway in *Ethanoligenens*. High lactate production in the High levels was due to up-expression of two pathways: pyruvate reduction by *Bifidobacterium* and the methylglyoxal bypass by *Megasphaera*. Propionate production may also occur via two pathways, each of which were up-expressed in the Low levels. However, propionate was not produced as a significantly greater proportion of product COD in either the High or Low levels.

In addition to the metabolic changes associated with product formation, several other key metabolic functionalities changed expression in the system. *Bifidobacterium* up-expressed glycogen synthesis in the Low levels, suggesting high substrate competition during the substrate-limited condition. In the High levels, *Bifidobacterium* up-expressed glucose uptake, glycolysis, and electron mediation. *Megasphaera* up-expressed glucose uptake in the High levels and electron mediation in the Low levels. Additionally, glycerol appears to have been produced by *Megasphaera* and consumed by *Clostridium* in the Low levels, though it was not detected in the product spectrum.

4.3. Lactate Production is Triggered by Expression of the Methylglyoxal Bypass

The change from HBU-type fermentation in the Low levels to HLa-type fermentation in the High levels appears largely attributable to the change in metabolic activity of *Megasphaera* (Fig. 6). During HLa-type fermentation, *Megasphaera* down-expressed enzymes involved in butyrate formation, pyruvate oxidation, and a number of flavoproteins and oxidases involved in electron mediation. Additionally, *Megasphaera* changed activity in the glycolysis side-branch pathways from lactate reduction and glycerol production to lactate generation via up-expression of glyoxylase, which removes methylglyoxal by hydration to lactate (Hoelzle et al., 2014). Methylglyoxal is a toxic byproduct of glycolysis which is produced from dihydroxyacetone-P when glucose consumption outpaces phosphate uptake (Booth et al., 2003; Ferguson, Totemeyer, MacLean, & Booth, 1998). It is hypothesized that methylglyoxal forms under these conditions as a mechanism to slow down substrate consumption by requiring the cell to spend energy detoxifying methylglyoxal to lactate. This mechanism is consistent with the observed increase in substrate uptake activity of *Megasphaera*

and corresponding decrease in relative abundance. The required redirection of cellular energy also agrees with the observed decrease in activity for electron mediation and production of butyrate and propionate by *Megasphaera* during up-expression of the methylglyoxal bypass. Given that phosphate is supplied in excess and the rest of the community did not show the same response, *Megasphaera* may have a less efficient phosphate uptake mechanism than other species. However, no direct evidence of limited *Megasphaera* phosphate uptake could be discerned from the metaproteome or from the literature.

In addition to the increased methylglyoxal bypass activity and subsequent reduction of the *Megasphaera* abundance, *Bifidobacterium* also increased lactate production activity in the High levels. Increased expression of this pathway was matched by increased glucose uptake, glycolysis, and electron mediation activity. This suggests that lactate production in *Bifidobacterium* was increased as a means to sink the excess electrons resulting from increased glucose oxidation when glucose was no longer limiting (Table 1).

A CCA of the entire proteome (including L5a) confirms that variation in lactate production though the operational levels is positively associated to increased expression of both lactate synthesis and especially the methylglyoxal bypass (Fig. 7). Additionally, the inverse relationship along CCA1 between lactate formation and expression of the lactate-consuming acrylate pathway of propionate formation highlights the other key metabolic shift away from lactate consumption. *Megasphaera* is known to reduce lactate to propionate as an electron sink, and will preferentially consume lactate through this pathway when available (Hino & Kuroda, 1993; Hino, Shimada, & Maruyama, 1994). The combination of down-expression of this pathway with the decreased abundance of *Megasphaera* in the High levels greatly reduced the effect of this lactate-consuming mechanism. Together, these correlations confirm that HLa-type fermentation was initiated by a decline in the butyrate-producing and lactate-consuming *Megasphaera* population resulting from expression of the methylglyoxal bypass.

4.4. Hexanoate Production in Level 5a

While the major products formed in L5a were similar to L10 and L5b, they were each produced at about 10 COD% lower yield in L5a (Fig. 1). Meanwhile, hexanoate was produced at about 10x higher yield in L5a. The co-dominance of *Ethanoligenens* and *Megasphaera* in this level (Fig. 2) suggests that this product spectrum divergence is community-linked rather than an expression difference within the same community.

Megasphaera is known to produce hexanoate via chain elongation through the reverse β -oxidation pathway, which utilizes butyrate pathway enzymes and their analogues to elongate ethanol and acetate to butyrate, hexanoate, and other high-carbon organic acids (Aglar et al., 2011; Spirito et al., 2014). Comparing the enzyme expression of L5a to L5b confirms that there was no significant difference in expression of butyrate pathway enzymes between levels 5a and 5b (Supplementary Fig. 7). The expressed functionalities that do change between L5a and L5b are the up-expression of electron mediation and acetate synthesis in L5a, and oxidative stress in L5b. The up-expressed acetate functionality is from *Ethanoligenens*. Although ethanol synthesis enzymes were not identified in this study, it is likely that this functionality was also up-expressed by *Ethanoligenens* in L5a due to this lineage's use of ethanol as an electron sink during acetate production (Castro et al., 2013; Xing et al., 2006). *Ethanoligenens* therefore seems the likely source of the chain elongation substrates acetate and ethanol. Use of reverse β -oxidation to elongate butyrate to hexanoate could therefore have been induced by the availability of chain elongation substrates rather than any change in expression of the butyrate/reverse β -oxidation pathway enzymes.

Conclusions

The reliable transition between sustained butyrate and lactate production at pH 5.5 was demonstrated by shifting from substrate limited to non-limited conditions. This represents a new MCF production mode for lactate, a high-value biopolymer feedstock chemical. The product transition corresponded with a change in the community profile resulting from expression of the methylglyoxal bypass in *Megasphaera* during high substrate loads. This metabolic mechanism can be included in future MCF models to describe the changes in product generation in substrate non-limiting conditions, and points to the important interplay between MCF conditions, community structure, and product profile. Furthermore, the protein expression profiles suggested

a likely syntrophic relationship between *Ethanoligenens* and *Megasphaera* in chain elongation via reverse β -oxidation to generate hexanoate at the lowest substrate concentration, though hexanoate production was not recoverable.

Combined metabolite and community profile analyses alone were not sufficient to uncover these mechanisms, and incorporation of expressional analysis through metaproteomics proved critical. While the metaproteome and community profiles could be linked for major lineages, future incorporation of metagenomes would likely uncover additional mechanisms by enabling creation of a custom protein database.

Acknowledgements

The authors would like to thank Christy Grobber for assistance with protein extractions, Amanda Nouwens for assistance with protein identification, and Yang Lu for assistance with community profiling. The authors declare no competing financial interests.

This study was supported by the Australian Research Council's Discovery Projects funding scheme (project number DP0985000). RH acknowledges support from the American Australian Association Sustainability Fellowship.

References

- Agler, M. T., Wrenn, B. A., Zinder, S. H., & Angenent, L. T. (2011). Waste to bioproduct conversion with undefined mixed cultures: the carboxylate platform. *Trends Biotechnol* , 29 (2), 70–78. <https://doi.org/10.1016/j.tibtech.2010.11.006>
- Alves de Oliveira, R., Komesu, A., Vaz Rossell, C. E., & Maciel Filho, R. (2018). Challenges and opportunities in lactic acid bioprocess design—From economic to production aspects. *Biochemical Engineering Journal* , 133 , 219–239. <https://doi.org/10.1016/j.bej.2018.03.003>
- Angenent, L. T., Karim, K., Al-Dahhan, M. H., Wrenn, B. a, & Domíguez-Espinosa, R. (2004). Production of bioenergy and biochemicals from industrial and agricultural wastewater. *Trends in Biotechnology* , 22 (9), 477–485. <https://doi.org/10.1016/j.tibtech.2004.07.001>
- Angenent, L. T., Richter, H., Buckel, W., Spirito, C. M., Steinbusch, K. J., Plugge, C., ... Hamelers, H. V. M. (2016). Chain elongation with reactor microbiomes: open-culture biotechnology to produce biochemicals. *Environmental Science & Technology* , acs.est.5b04847. <https://doi.org/10.1021/acs.est.5b04847>
- Atasoy, M., Eyice, O., Schnürer, A., & Cetecioglu, Z. (2019). Volatile fatty acids production via mixed culture fermentation: Revealing the link between pH, inoculum type and bacterial composition. *Bioresource Technology* , 292 (July), 121889. <https://doi.org/10.1016/j.biortech.2019.121889>
- Bastidas-Oyanedel, J. R., Mohd-Zaki, Z., Pratt, S., Steyer, J. P., & Batstone, D. J. (2010). Development of membrane inlet mass spectrometry for examination of fermentation processes. *Talanta* , 83 (2), 482–492. <https://doi.org/10.1016/j.talanta.2010.09.034>
- Bateman, A., Martin, M. J., O'Donovan, C., Magrane, M., Apweiler, R., Alpi, E., ... Zhang, J. (2015). UniProt: a hub for protein information. *Nucleic Acids Research* , 43 (D1), D204–D212. <https://doi.org/10.1093/nar/gku989>
- Booth, I. R., Ferguson, G. P., Miller, S., Li, C., Gunasekera, B., & Kinghorn, S. (2003). Bacterial production of methylglyoxal: a survival strategy or death by misadventure? *Biochemical Society Transactions* , 31 (Pt 6), 1406–1408. <https://doi.org/10.1042/>
- Caporaso, J. G., Kuczynski, J., Stombaugh, J., Bittinger, K., Bushman, F. D., Costello, E. K., ... Knight, R. (2010). QIIME allows analysis of high-throughput community sequencing data. *Nature Methods* , 7 (5), 335–336. <https://doi.org/10.1038/nmeth.f.303>
- Castro, J. F., Razmilic, V., & Gerdtzen, Z. P. (2013). Genome based metabolic flux analysis of *Ethanoligenens harbinense* for enhanced hydrogen production. *International Journal of Hydrogen Energy* , 38 (3), 1297–1306.

<https://doi.org/10.1016/j.ijhydene.2012.11.007>

Choi, M., Chang, C.-Y., Clough, T., Broudy, D., Killeen, T., MacLean, B., & Vitek, O. (2014). MSstats: an R package for statistical analysis of quantitative mass spectrometry-based proteomic experiments. *Bioinformatics* , 30 (17), 2524–2526. <https://doi.org/10.1093/bioinformatics/btu305>

Dams, R. I., Viana, M. B., Guilherme, A. A., Silva, C. M., dos Santos, A. B., Angenent, L. T., ... Leitão, R. C. (2018). Production of medium-chain carboxylic acids by anaerobic fermentation of glycerol using a bioaugmented open culture. *Biomass and Bioenergy* ,118 (August), 1–7. <https://doi.org/10.1016/j.biombioe.2018.07.023>

De Groof, V., Coma, M., Arnot, T., Leak, D. J., & Lanham, A. B. (2019). Medium chain carboxylic acids from complex organic feedstocks by mixed culture fermentation. *Molecules* , 24 (3), 1–32. <https://doi.org/10.3390/molecules24030398>

de Vries, W., & Stouthamer, A. H. (1968). Fermentation of Glucose, Lactose, Galactose, Mannitol, and Xylose by Bifidobacteria. *Journal of Bacteriology* , 96 (2), 472–478. <https://doi.org/10.1128/JB.96.2.472-478.1968>

El-Mansi, E. M. T., Bryce, C. F. A., Demain, A. L., & Allman, A. R. (2006). *Fermentation Microbiology and Biotechnology* (2nd ed.). Boca Raton, Florida, USA: CRC Press.

Eng, S. C., Fernandes, X. A., & Paskins, A. R. (1986). Biochemical effects of administering shock loads of sucrose to a laboratory-scale anaerobic (UASB) effluent treatment plant. *Water Research* ,20 (6), 789–794. [https://doi.org/10.1016/0043-1354\(86\)90105-3](https://doi.org/10.1016/0043-1354(86)90105-3)

Engelbrektson, A., Kunin, V., Wrighton, K. C., Zvenigorodsky, N., Chen, F., Ochman, H., & Hugenholtz, P. (2010). Experimental factors affecting PCR-based estimates of microbial species richness and evenness. *The ISME Journal* , 4 (5), 642–647. <https://doi.org/10.1038/ismej.2009.153>

Ferguson, G. P., Töttemeyer, S., MacLean, M. J., & Booth, I. R. (1998). Methylglyoxal production in bacteria: suicide or survival? *Archives of Microbiology* , 170 (4), 209–218. <https://doi.org/10.1007/s002030050635>

González-Cabaleiro, R., Lema, J. M., & Rodríguez, J. (2015). Metabolic energy-based modelling explains product yielding in anaerobic mixed culture fermentations. *PLoS ONE* , 10 (5), 1–17. <https://doi.org/10.1371/journal.pone.0126739>

Gonzalez-Garcia, R. A., McCubbin, T., Navone, L., Stowers, C., Nielsen, L. K., & Marcellin, E. (2017). Microbial propionic acid production. *Fermentation* , 3 (2), 1–20. <https://doi.org/10.3390/fermentation3020021>

Grobber, C., Viridis, B., Nouwens, A., Harnisch, F., Rabaey, K., & Bond, P. L. (2014). Use of SWATH mass spectrometry for quantitative proteomic investigation of *Shewanella oneidensis* MR-1 biofilms grown on graphite cloth electrodes. *Systematic and Applied Microbiology* , 1–5. <https://doi.org/10.1016/j.syapm.2014.11.007>

Hino, T., & Kuroda, S. (1993). Presence of lactate dehydrogenase and lactate racemase in *Megasphaera elsdenii* grown on glucose or lactate. *Applied and Environmental Microbiology* , 59 (1), 255–259. <https://doi.org/10.1128/AEM.59.1.255-259.1993>

Hino, T., Shimada, K., & Maruyama, T. (1994). Substrate Preference in a Strain of *Megasphaera elsdenii*, a Ruminant Bacterium, and Its Implications in Propionate Production and Growth Competition. *Applied and Environmental Microbiology* , 60 (6), 1827–1831. <https://doi.org/10.1128/AEM.60.6.1827-1831.1994>

Hoelzle, R. D., Viridis, B., & Batstone, D. J. (2014). Regulation mechanisms in mixed and pure culture microbial fermentation. *Biotechnology and Bioengineering* , 111 (11), 2139–2154. <https://doi.org/10.1002/bit.25321>

Hofvendahl, K., & Hahn-Hägerdal, B. (2000). Factors affecting the fermentative lactic acid production from renewable resources. *Enzyme and Microbial Technology* , 26 (2–4), 87–107. [https://doi.org/10.1016/S0141-0229\(99\)00155-6](https://doi.org/10.1016/S0141-0229(99)00155-6)

- Jang, Y.-S., Kim, B., Shin, J. H., Choi, Y. J., Choi, S., Song, C. W., ... Lee, S. Y. (2012). Bio-based production of C2-C6 platform chemicals. *Biotechnology and Bioengineering* , 109 (10), 2437–2459. <https://doi.org/10.1002/bit.24599>
- Juste-Poinapen, N. M. S., Turner, M. S., Rabaey, K., Viridis, B., & Batstone, D. J. (2015). Evaluating the potential impact of proton carriers on syntrophic propionate oxidation. *Scientific Reports* , 5 , 18364. <https://doi.org/10.1038/srep18364>
- Kucek, L. A., Spirito, C. M., & Angenent, L. T. (2016). High n-caprylate productivities and specificities from dilute ethanol and acetate: Chain elongation with microbiomes to upgrade products from syngas fermentation. *Energy and Environmental Science* , 9 (11), 3482–3494. <https://doi.org/10.1039/c6ee01487a>
- Lu, Y., Slater, F. R., Mohd-Zaki, Z., Pratt, S., & Batstone, D. J. (2011). Impact of operating history on mixed culture fermentation microbial ecology and product mixture. *Water Science & Technology* , 64 (3), 760. <https://doi.org/10.2166/wst.2011.699>
- Marounek, M., Fliegerova, K., & Bartos, S. (1989). Metabolism and some characteristics of ruminal strains of *Megasphaera elsdenii*. *Applied and Environmental Microbiology* , 55 (6), 1570–1573.
- Matallana-Surget, S., Jagtap, P. D., Griffin, T. J., Beraud, M., & Wattiez, R. (2017). *Comparative Metaproteomics to Study Environmental Changes . Metagenomics: Perspectives, Methods, and Applications* . Elsevier Inc. <https://doi.org/10.1016/B978-0-08-102268-9.00017-3>
- Mohd-Zaki, Z., Bastidas-Oyanedel, J., Lu, Y., Hoelzle, R., Pratt, S., Slater, F., & Batstone, D. (2016). Influence of pH Regulation Mode in Glucose Fermentation on Product Selection and Process Stability. *Microorganisms* , 4 (1), 2. <https://doi.org/10.3390/microorganisms4010002>
- Rodriguez, J., Kleerebezem, R., Lema, J. M., & van Loosdrecht, M. C. (2006). Modeling product formation in anaerobic mixed culture fermentations. *Biotechnol Bioeng* , 93 (3), 592–606. <https://doi.org/10.1002/bit.20765>
- Romli, M., Keller, J., Lee, P. L., & Greenfield, P. F. (1995). Model prediction and verification of a two-stage high-rate anaerobic wastewater treatment system subjected to shock loads. *Process Safety and Environmental Protection* , 73 (2), 151–154.
- Singleton, C., McCalley, C., Woodcroft, B., Boyd, J., Evans, P., Hodgkins, S., ... Tyson, G. (2018). Methanotrophy across a natural permafrost thaw environment. *ISME Journal* , 1 . <https://doi.org/10.1038/s41396-018-0065-5>
- Spirito, C. M., Marzilli, A. M., & Angenent, L. T. (2018). Higher Substrate Ratios of Ethanol to Acetate Steered Chain Elongation toward n-Caprylate in a Bioreactor with Product Extraction. *Environmental Science and Technology* , 52 , 13438–13447. research-article. <https://doi.org/10.1021/acs.est.8b03856>
- Spirito, C. M., Richter, H., Rabaey, K., Stams, A. J. M., & Angenent, L. T. (2014). Chain elongation in anaerobic reactor microbiomes to recover resources from waste. *Current Opinion in Biotechnology* , 27 , 115–122. <https://doi.org/10.1016/j.copbio.2014.01.003>
- Temudo, M F, Muyzer, G., Kleerebezem, R., & van Loosdrecht, M. C. (2008). Diversity of microbial communities in open mixed culture fermentations: impact of the pH and carbon source. *Appl Microbiol Biotechnol* , 80 (6), 1121–1130. <https://doi.org/10.1007/s00253-008-1669-x>
- Temudo, Margarida F, Kleerebezem, R., & van Loosdrecht, M. (2007). Influence of the pH on (open) mixed culture fermentation of glucose: a chemostat study. *Biotechnol Bioeng* , 98 (1), 69–79. <https://doi.org/10.1002/bit.21412>
- Voolapalli, R. (2001). Hydrogen production in anaerobic reactors during shock loads—influence of formate production and H₂ kinetics. *Water Research* , 35 (7), 1831–1841. [https://doi.org/10.1016/S0043-1354\(00\)00441-3](https://doi.org/10.1016/S0043-1354(00)00441-3)

Wang, X., & Kuruc, M. (2019). *Functional Proteomics: Methods and Protocols*. (X. Wang & M. Kuruc, Eds.) (Vol. 1871). New York, NY: Springer New York. <https://doi.org/10.1007/978-1-4939-8814-3>

Watier, D., Dubourguier, H. C., Leguerinel, I., & Hornez, J. P. (1996). Response Surface Models To Describe the Effects of Temperature, pH, and Ethanol Concentration on Growth Kinetics and Fermentation End Products of a *Pectinatus* sp. *Applied and Environmental Microbiology*, *62* (4), 1233–1237. <https://doi.org/10.1128/AEM.62.4.1233-1237.1996>

Weimer, P. J., & Moen, G. N. (2013). Quantitative analysis of growth and volatile fatty acid production by the anaerobic ruminal bacterium *Megasphaera elsdenii* T81. *Applied Microbiology and Biotechnology*, *97* (9), 4075–4081. <https://doi.org/10.1007/s00253-012-4645-4>

Widdel, F., & Bak, F. (1992). Gram-Negative Mesophilic Sulfate-Reducing Bacteria. In *The Prokaryotes* (pp. 3352–3378). New York, NY: Springer New York. https://doi.org/10.1007/978-1-4757-2191-1_21

Wolin, M. J., Zhang, Y., Bank, S., Yerry, S., & Miller, T. L. (1998). NMR detection of 13CH₃13COOH from 3-13C-glucose: a signature for *Bifidobacterium* fermentation in the intestinal tract. *J Nutr*, *128* (1), 91–96. <https://doi.org/10.1093/jn/128.1.91>

Woodcroft, B. J., Singleton, C. M., Boyd, J. A., Evans, P. N., Emerson, J. B., Zayed, A. A. F., ... Tyson, G. W. (2018). Genome-centric view of carbon processing in thawing permafrost. *Nature*. <https://doi.org/10.1038/s41586-018-0338-1>

Xing, D., Ren, N., Li, Q., Lin, M., Wang, A., & Zhao, L. (2006). *Ethanoligenens harbinense* gen. nov., sp. nov., isolated from molasses wastewater. *International Journal of Systematic and Evolutionary Microbiology*, *56* (4), 755–760. <https://doi.org/10.1099/ijs.0.63926-0>

Figure Legends

Figure 1: Time-course product data of the steady state periods by COD composition. Confidence intervals for major products at each level were consistently [?]10% of the mean. Vertical bars separate the individual operational levels.

Figure 2: Heatmap of square root-transformed relative abundance of genus-aggregated lineages, as well as the level Shannon diversity index (H), each averaged across all samples from each operational level. Genera with relative abundance of <0.50% are aggregated into “Other”. All labelled taxa are from the Bacteria domain. The dendrogram and Shannon diversity are based on the non-aggregated community profile.

Figure 3: CCA of the genus-aggregated 16S rDNA community and protein abundance profiles across operational levels. Only the 10 most abundant genera (averaged between both the community and protein data sets) are highlighted. Individual 16S rDNA genus aggregates are plotted as grey points with highlighted genera as orange Xs and labelled in italic text. Highlighted protein genus aggregates are plotted as vectors and labelled in greyed text. Non-highlighted proteins are not shown. Individual samples are plotted by color and shape according to their operational level. Protein samples without corresponding community samples were not used.

Figure 4: Volcano plot depicting significant expressional changes of all identified carbon energy metabolism proteins. Expression comparison is represented on the horizontal axis as log₂-fold change (L2FC) between Low (blue, negative L2FC values) and High (red, positive L2FC values) levels. Significance is represented on the vertical axis as the -log₁₀ of the adjusted p-value from MSstats ‘groupComparison’ output, where p = 0.05 is plotted as a dashed line at 1.30. Points above the line (p < 0.05) are considered statistically significant. Proteins are categorized by pathway or metabolic function as represented by shape and described in the key. Proteins from key pathways (acetate, butyrate, lactate, and substrate uptake) are labelled according to the lineage they were found in.

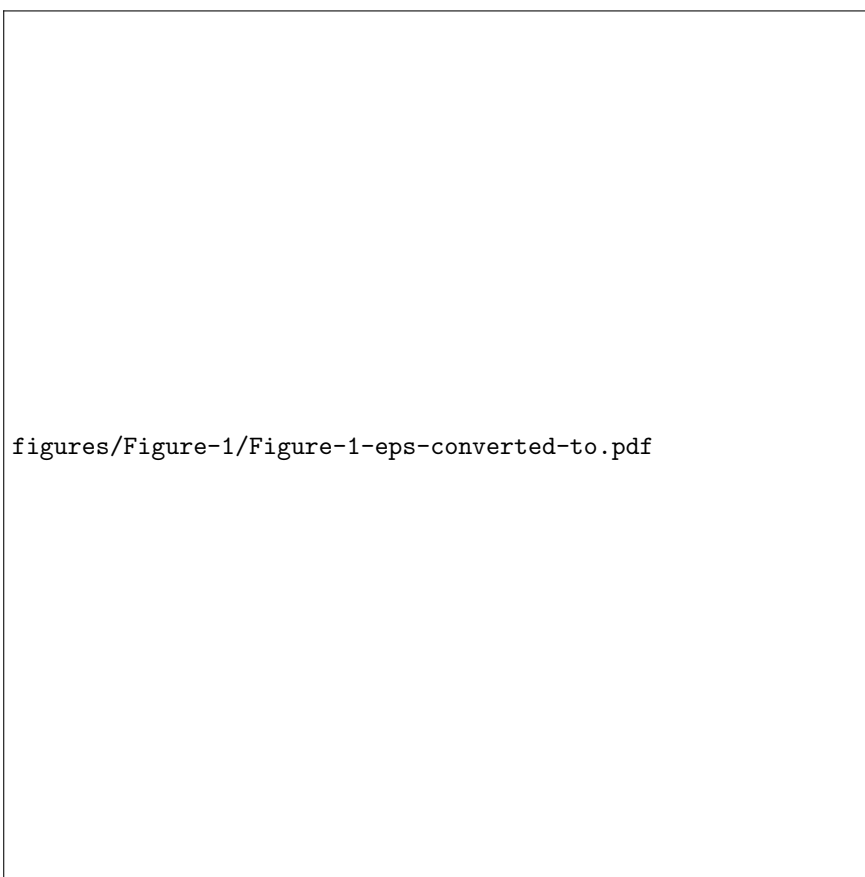
Figure 5: Expression map of mixed culture carbon and energy metabolism. Text color indicates the condition under which the product is more highly produced. L2FC for significantly up-expressed proteins

from each pathway were averaged separately within the High and Low conditions. The higher of the two averages is represented by arrow color and width, and the lineages responsible for the up-expression are labelled next to the pathway. Arrows representing glucose uptake and electron mediation functions, having clear lineage differentiation between High and Low levels, are shown for both conditions.

Figure 6: CCA of pathway expression and product concentrations. Individual metabolic pathways are plotted as grey points, and select carbon metabolism pathways highlighted with black symbols. Genus-normalized protein abundances were averaged for each pathway category (Supplementary Table 3) within each sample to generate the pathway expression data. Products are plotted as vectors and labelled accordingly. Individual samples are plotted by color and shape according to their operational level.

Hosted file

Table 1.docx available at <https://authorea.com/users/350167/articles/475076-lactate-vs-butyrate-production-during-mixed-culture-glucose-fermentation-driven-by-substrate-availability-as-determined-by-metaproteomics>



figures/Figure-2/Figure-2-eps-converted-to.pdf

figures/Figure-3/Figure-3-eps-converted-to.pdf

figures/Figure-4/Figure-4-eps-converted-to.pdf

figures/Figure-5/Figure-5-eps-converted-to.pdf

figures/Figure-6/Figure-6-eps-converted-to.pdf